iAAA-mitochondrial protease YME1L1 regulates the degradation of short-lived mitochondrial transporter SLC25A38

Sijie Tan[1], Nora Kory[1,2]*

[1]Department of Molecular Metabolism, Harvard T.H. Chan School of Public Health, Boston, MA, USA
[2]Dana-Farber Cancer Institute, Boston, MA, USA

***Corresponding author.** Email: nkory@hsph.harvard.edu

ABSTRACT

Mitochondrial transporters facilitate the exchange of diverse metabolic intermediates across the inner mitochondrial membrane to ensure adequate amounts of substrates and cofactors to support the redox and biosynthetic reactions in the mitochondrial matrix. However, how the abundance of mitochondrial transporters is regulated and the mechanisms controlling mitochondrial metabolite concentrations remain poorly defined. Using protein half-life data and mRNA-protein correlation analysis, we identify SLC25A38, a mitochondrial glycine transporter, as a short-lived protein, whose mitochondrial pool is turned over with a half-life of 4 hours under steady-state conditions. Pharmacological inhibition and genetic depletion of different cellular proteolytic systems revealed that proteasomal and lysosomal systems do not affect the stability of SLC25A38. Instead, we found that the mitochondrial iAAA-protease YME1L1 regulates the abundance and turnover of SLC25A38 under steady-state conditions. Identification of YME1L1 as the molecular player that regulates SLC25A38 levels will open up avenues to explore how cells coordinate mitochondrial substrate uptake with heme synthesis and other glycine-dependent mitochondrial metabolic pathways under physiological state or in response to environmental cues.

INTRODUCTION

Mitochondria are metabolic hubs for energy production, biosynthetic processes, and redox reactions[1]. Transport proteins including members of the SoLute Carrier 25 (SLC25) family facilitate the transport of metabolites across the inner mitochondrial membrane (IMM) to ensure adequate concentrations of critical substrates and cofactors in the mitochondrial matrix to support these reactions[2]. How cells coordinate the abundance and activity of SLC25 transporters with their metabolic requirements and control mitochondrial metabolite pools remains poorly defined.

Heme is a vital cofactor for diverse redox processes such as oxygen transport, mitochondrial respiration, and detoxification[3]. Heme synthesis is highly compartmentalized between mitochondria and the cytosol and multiple steps of the eight enzymatic reactions require the shuttling of substrates across the IMM[4]. The first step involves the uptake of glycine into the mitochondrial matrix via SLC25A38[5,6], where glycine is condensed with succinyl-CoA to produce 5-aminolevulinate (5-ALA). 5-ALA is subsequently exported to the cytosol and converted to coproporphyrinogen III (CPgenIII) through a series of reactions. The last few steps of heme synthesis occur in the mitochondrial matrix and require the transport of CPgenIII to the intermembrane space via ABCB6, where additional reactions will generate protoporphyrin IX (PPIX). PPIX is transported to the matrix via TMEM14C and combines with iron to form heme. Mutations in enzymes or transporters involved in heme synthesis[7], including SLC25A38, ALA synthase 2, and ABCB7, cause congenital sideroblastic anemia, a condition characterized by mitochondrial iron accumulation in erythroblasts due to dysfunctional heme synthesis or processing.

Heme synthesis requires the coordination of multiple metabolic steps and is tightly controlled due to the inherent toxicity of metabolic intermediates and free heme[8]. However, how the abundance of transporters coordinates with heme metabolism is not known. In this study, we mined protein half-life data and mRNA-protein abundance ratios to determine mitochondrial transporters whose abundance is regulated. We identify SLC25A38, a transporter involved in the first step of heme synthesis, as a short-lived mitochondrial transporter whose mitochondrial pool is rapidly turned over under physiological state, thus uncovering a new potential regulatory mechanism of heme synthesis.

RESULTS

SLC25A38 is a short-lived mitochondrial protein

To identify mitochondrial transporters whose abundance is regulated, we compared the protein and mRNA levels of SLC25 transporters using information from OpenCell[9]. While for most SLC25 transporters, protein-to-mRNA abundance ratios followed the correlation seen in the general proteome, SLC25A23, SLC25A35, SLC25A38, SLC25A39, and SLC25A42 exhibited low protein-to-mRNA ratios (Fig. 1a), suggesting that the synthesis or degradation of these proteins might be regulated. Indeed, SLC25A39, the mitochondrial glutathione (GSH) transporter[10,11], was recently reported as a short-lived protein whose levels are controlled by regulated proteolysis[12,13]. We focused on SLC25A38, a transporter involved in the highly regulated heme synthesis process, and hypothesized that SLC25A38 protein is also rapidly turned over under steady-state conditions. To affirm this hypothesis, we mined published proteomics datasets for half-life data on SLC25 transporters. High throughput quantitative proteomics to measure protein degradation kinetics mapped SLC25A38 as a short-lived protein in human cell lines under basal condition[14,15] (Fig. 1b). To measure the half-life of SLC25A38 in HEK293T cells, we blocked protein synthesis using cycloheximide (CHX) and determined SLC25A38 protein levels overtime ('chase') by western blot (Fig. 1c). We observed that endogenous and stably expressed FLAG-tagged SLC25A38 had a half-life of ~4 hrs (Fig. 1c), which is significantly shorter than the median half-life of mitochondrial carriers in mammalian cells of several days (Fig. 1b). Conversely, SLC25A51, a mitochondrial NAD^+ transporter[16-18], which showed similar protein-to-mRNA abundance as the general proteome exhibited a half-life of >8 hrs (Fig. 1c). This highlights that the turnover of SLC25A38 under basal conditions is specific to this transporter and not due to general destabilization of mitochondrial transporters by CHX. To further ascertain if the rapid degradation of SLC25A38 was due to the removal of its mitochondrial pool, we blocked protein synthesis using CHX, fractionated cells at different time points post the start of CHX treatment into cytosolic versus mitochondrial fractions, and determined SLC25A38 protein in both fractions by western blot. We observed that endogenous and FLAG-tagged SLC25A38 were primarily present in the mitochondrial fraction and with subsequent CHX treatment, the protein levels decreased over time (Fig. 1d). Immunofluorescence imaging also highlighted the distinct localization of SLC25A38 to the mitochondria, with the signal decreasing upon CHX treatment (Fig. 1e). These observations indicate SLC25A38 is a short-lived mitochondrial protein under physiological state due to rapid degradation.

Proteasomal and lysosomal systems do not regulate the stability or turnover of SLC25A38

We sought to determine the machinery involved in SLC25A38 degradation. We focused on the three major proteolytic systems that contribute to the degradation of mitochondrial proteins: (i) proteasome, (ii) lysosome (mitophagy), and (iii) mitochondrial proteases. Inhibition of the proteasome using bortezomib and epoxomicin did not impact SLC25A38 basal levels and stability (Fig. 2a). Likewise, inhibition of lysosomal acidification by NH_4Cl treatment or *Atg5* knockout (KO), which blocks

autophagy, did not alter SLC25A38 basal levels or turnover rate (Fig. 2b and c). These results highlight that the degradation of SLC25A38 is independent of mitophagy.

Mitochondrial iAAA protease YME1L1 degrades SLC25A38 basally

As an inner mitochondrial membrane protein, SLC25A38 is accessible to proteases present in the mitochondrial matrix, inner membrane, and intermembrane space, which include at least 20 catalytically functional proteases that participate in cellular stress signaling and proteostasis[19,20]. To investigate the contribution of mitochondrial proteases to SLC25A38 turnover, we deleted five major mammalian mitochondrial proteases using CRISPR and monitored SLC25A38 degradation in the CHX-chase assay. Deletion of AFG3L2, LONP1, CLPP, and PARL did not affect SLC25A38 levels or turnover (Fig. 3a). However, YME1L1 KO increased the steady-state levels of SLC25A38 and substantially extended the transporter half-life beyond 8 hrs (Fig. 3b). This suggests that YME1L1 regulates the rapid degradation of SLC25A38 basally.

DISCUSSION

SLC25 transporters comprise the largest solute carrier family in humans and import and export diverse solutes across the IMM[2]. They function as gatekeepers to compartmentalize and protect the intramitochondrial metabolite pools to create a chemically optimal environment to facilitate the numerous biochemical processes in the matrix. Regulating the levels of mitochondrial transporters could provide a means for control of mitochondrial metabolic content and activity[1]. However, the regulatory mechanisms that fine-tune transporter abundance to coordinate metabolic homeostasis remain unknown for most SLC25 transporters. Here, we report that the mitochondrial glycine transporter SLC25A38[5,6] is a short-lived protein, whose abundance is regulated by the iAAA-mitochondrial protease YME1L1. By coupling CHX-chase with pharmacological inhibition or genetic depletion of different cellular proteolysis machinery, our work confirmed that basal SLC25A38 stability and turnover rate depend on YME1L1. This is in line with a previously published proteomics dataset, in which SLC25A38 accumulates in YME1L1 knockout cells along with other YME1L1 substrates[21]. Thus, together with other recent studies, our work establishes degradation by mitochondrial proteases as a mechanism regulating the abundance of transporters in the inner mitochondrial membrane[12,13]. Further experiments are required to test whether YME1L1 directly degrades SLC25A38, or whether YME1L1 indirectly affects SLC25A38 stability through the degradation of other proteases[22,23], as has been reported for OMA1.

Heme synthesis is initiated exclusively in the mitochondria, and the first step requires the import of glycine into the mitochondrial matrix through SLC25A38[5,6]. Gene ontology annotations linked SLC25A38 to erythrocyte differentiation. Loss-of-function mutations in SLC25A38 cause congenital sideroblastic anemia[24], a condition likely driven by dysfunctional heme synthesis or processing in erythroblasts. Although heme is a cofactor for multiple redox processes in humans, excess free heme is deleterious due to its ability to promote oxidative stress and lipid peroxidation[8]. Hence, heme synthesis is tightly controlled or coupled to its utilization to prevent overt accumulation and cytotoxicity. We postulate that the short-lived nature of SLC25A38 allows the cell to respond rapidly to changing metabolic demands or heme levels and fine-tune heme synthesis through SLC25A38 degradation and transporter availability on the IMM while preventing the accumulation of potentially toxic heme synthesis intermediates. Interestingly, the proteolytic regulation of SLC25A38 mirrors that of SLC25A39, a mitochondrial GSH transporter that plays a role in erythropoiesis[25]. Works by Liu et. al[12]. and Shi et. al[13]. reported SLC25A39 is a short-lived protein rapidly degraded by mAAA-mitochondrial protease AFG3L2. This rapid proteolysis of SLC25A39 allows the mitochondria to coordinate GSH and iron metabolism to prevent cytotoxicity induced by excess iron[12,13]. Given the essential role of SLC25A38 and SLC25A39 in erythropoiesis, we believe the rapid degradation of these transporters may have evolved as a strategy for cells to cope with heme metabolism and concomitantly buffer against reactive metabolic intermediates. Although our work reports the regulation of SLC25A38 under a physiological state, the findings could open new avenues to understand the contribution of YME1L1-SLC25A38 interplay in physiological processes like erythropoiesis or pathological states linked to improper heme synthesis.

MATERIALS AND METHODS

Cell culture

HEK293T were cultured in DMEM high glucose with L-glutamine and sodium pyruvate supplemented with 10% FBS and 1% penicillin-streptomycin (Hyclone, Cytiva), unless stated otherwise. All cell lines were grown in 5% CO_2 at 37°C.

Lentivirus production and generation of stable cell lines

For lentivirus production, 400,000 HEK293T cells were seeded in a 6-well plate in DMEM with 20% IFS and 1% penicillin-streptomycin. After 24 hrs recovery, the cells were transfected with 1ug pMXs empty vector or 1ug pMXs-SLC25A38-3xFLAG, 900ng pCMV-Gag-Pol, and 150ng pCMV-VSVG using X-tremeGENE 9 DNA Transfection Reagent (Sigma) following manufacturer's protocol. 24 hrs later, the media was replaced with DMEM with 30% IFS and 1% penicillin-streptomycin. Another 24 hrs later, the supernatant was collected and filtered through 0.45 mm sterile filter. The virus was stored at -80ºC. For infection, 400,000 HEK293T cells were seeded in a 6-well plate. After 24 hrs recovery, the cells were infected with 300ul of virus and 10ug/ml polybrene (Millipore). After 48 hrs infection, the cells were selected with 10ug/ml blasticidin (Millipore) until the control well (without virus addition) reached 100% cell death. The empty vector-HEK293T and SLC25A38-3xFLAG-HEK293T stable cells were subsequently maintained in 2ug/ml blasticidin.

Cycloheximide (CHX)-chase assay

800,000 cells were seeded in a 6-well plate. After 24 hrs recovery, the cells were treated with 10ug/ml CHX (Sigma), or with the addition of 10nM bortezomib (MedChemExpress) or 50nM epoxomicin (MedChemExpress) or 20mM NH_4Cl (Sigma), and harvested at the indicated time points.

Protein lysis and immunoblotting

Cells were lysed in RIPA buffer (Thermo Scientific) supplemented with 1x Halt Protease and Phosphatase Inhibitor Cocktail (Thermo Scientific). The cells were lysed on ice for 20 min with intermittent vortexing followed by centrifugation at 14,000 rpm for 15 min at 4°C. Supernatants were collected. Cellular fractionation into cytosolic and mitochondrial fractions were done with the Mitochondria Isolation Kit for Cultured Cells (Thermo Scientific) following manufacturer's protocol. Protein concentrations were determined with Pierce BCA Protein Assay Kit (Thermo Scientific). SDS-PAGE and wet transfer western blotting were performed and the blots were labelled with Pierce™ ECL Western Blotting Substrate (Thermo Scientific) and imaged with Bio-Rad ChemiDoc MP imaging system.

The following antibodies and dilutions were used: β-Actin (13E5) HRP conjugate (Cell signalling #5125; 1:10,000), FLAG (M2) (Sigma F1804; 1:1000), SLC25A38 (Abcam ab133614; 1:1000), SLC25A51 (Novus NBP2-46847; 1:1000), TOMM20 (Proteintech 11802-1-AP; 1:1000), anti-rabbit IgG HRP-linked antibody (Cell signalling 7074; 1:10,000), anti-mouse IgG HRP-linked antibody (Cell signalling 7076; 1:10,000).

Immunofluorescence

200,000 cells were seeded onto poly-D-lysine coated coverslips (Neuvitro). After 24 hrs recovery, the cells were treated 10ug/ml CHX and fixed with 3% paraformaldehyde (Sigma) and 0.1% glutaraldehyde (Sigma) for 10 min at the indicated time points. Subsequently, the cells were permeabilized and blocked using buffer containing 0.2% milk, 2% FBS, 1% BSA, and 0.01% triton X-100. The cells were stained with F and citrate synthase (D7V8B) (Cell signalling #14309) antibodies (1:300 dilution) overnight followed by Abberior STAR secondary antibodies (1:800 dilution) for 2 hrs. Coverslips were mounted onto slide with Prolonged Gold Antifade Medium containing DAPI (Invitrogen). Images were acquired with Zeiss spinning disk confocal microscope using the 100x oil immersion objective lens. 10 random fields per coverslip were imaged and the same acquisition parameters were applied to all conditions.

Cloning single-guide RNA (sgRNA) into pX330

sgRNAs were designed using the Synthego Knockout Guide Designer tool. sgRNA sequences are reported in table 1. Forward and reverse sgRNA oligos were annealed at 95°C for 5 min followed by slow cooling to 4°C. pX330 (Addgene) was digested with *BbsI*. The linearized pX330 was separated on a DNA agarose gel and the band was excised and purified with QIAquick Gel Extraction Kit (Qiagen). Annealed oligos were ligated with linearized pX330 at room temperature overnight with T4 ligase (NEB). Ligated products were transformed into DH5α and positive clones were confirmed by sanger sequencing.

Table 1: sgRNA sequence for mitochondrial proteases

Mitochondrial protease	Forward and reverse sequences (5' to 3')
AFG3L2	F: GCTACCACACGCTCTTCTGG R: CCAGAAGAGCGTGTGGTAGC
LONP1	F: CTTCTCCCACAGCAATGAGT R: ACTCATTGCTGTGGGAGAAG
CLPP	F: CACAGGTGGTGTGGTGACCG R: CGGTCACCACACCACCTGTG
PARL	F: GTCCCTGGGTCTGATCTTCG R: CGAAGATCAGACCCAGGGAC
YME1L1	F: AGTGTTTTTTGGTGTATGGA R: TCCATACACCAAAAAACACT

CRISPR knockout (KO) of mitochondrial proteases

300,000 cells were seeded in a 6-well plate. After 24 hrs, recovery, the cells were transfected with 2ug pX330-sgRNA and 0.2ug of GFP empty vector using Lipofectamine 3000 (Invitrogen) at 1:3 DNA to lipofectamine ratio following manufacturer's protocol. After 48 hrs transfection, the cells were harvested and GFP+ cells were sorted into single-cell in a 96-well plate using BD FACSAria Cell Sorter. After 2-3 weeks, single-cell colonies were transferred to 6-well plates and genomic DNA was extracted after the cells reached ~80% confluency. PCR was performed with the genomic DNA using

primers (forward and reverse) at least 150 bp from the sgRNA cut-site and to yield PCR amplicon between 400-800 bp. PCR products were purified and sent for sanger sequencing. Sequencing results were analysed with Synthego Inference of CRISPR Edits (ICE) tool and positive KO clones were further confirmed with next-generation sequencing.

Analysis

For western blots, densitometric analysis of the protein bands was performed using Image J. For CHX-chase, relative protein abundance at the different time points were normalized to the first time point (0 hrs). For immunofluorescence, 10 images totalling to 200-400 cells were analysed for the average FLAG and citrate synthase signals at each time point using Image J. All results were plotted as mean + standard deviation mean. Student's t-test was used to determine statistical significance, defined by $*p$ value <0.05 and $**p$ value <0.01.

FIGURE LEGENDS

Figure 1: SLC25A38 is a short-lived mitochondrial transporter with a half-life of ~4 hrs. (a) Scatterplot from OpenCell[8] showing the protein and mRNA abundance of all proteins expressed in HEK293T cells. Red region highlights proteins with low protein-to-mRNA ratio based on cut-off ratio of ~0.5. Green region highlights high protein-to-mRNA ratio based on cut-off ratio of 2.0. (b) Half-life of SLC25 transporters in HeLa and Huh7 cells. Graph is plotted with data extracted from Human mitochondrial high-confidence proteome (MitoCoP[9]). Dotted line indicates the median half-life of mitochondrial transporters. (c) Relative protein abundance of endogenous and FLAG-expressing SLC25A38, and endogenous SLC25A51 at different CHX treatment time points normalized to the protein abundance at 0 hrs (n = 3). For SLC25A51, the levels in SLC25A38-3xFLAG-HEK293T were plotted. (d) Cytosolic and mitochondrial levels of endogenous and FLAG-expressing SLC25A38 at different CHX treatment time points. TOMM20 and actin were controls to indicate purity of cellular fractionation (n = 1). (e) Quantification of FLAG and citrate synthase (CS) signals in SLC25A38-3xFLAG-HEK293T under 0 and 8 hrs CHX treatment. 10 images totalling to 200-400 cells for each time point were quantified to calculate the average FLAG and CS intensity. Scale bar = 10um. Values are mean ± S.D.M.

Figure 2: Proteasomal and lysosomal inhibition, and *Atg5* knockout did not affect SLC25A38 degradation basally. (a-b) Relative endogenous SLC25A38 levels at different CHX treatment time points under basal condition (untreated), proteasomal inhibition with bortezomib or epoxomycin, or lysosomal inhibition with NH_4Cl. Fold change values were normalized to the protein abundance at 0 hrs (n = 2 for a, n = 1 or b). (c) Relative endogenous SLC25A38 levels in WT and *Atg5* KO HEK293T with and without CHX treatment for 16 hrs (n = 3). Cropped blots were from the same gel. Fold change values were normalized to WT -CHX. Values are mean ± S.D.M.

Figure 3: YME1L1 regulates SLC25A38 degradation basally. (a) Relative endogenous SLC25A38 levels in non-targeting KO control (sgAAVS1) and mitochondrial protease CRISPR KO cells at different time points of CHX treatment, normalized to the protein abundance at 0 hrs. 1 or 2 KO clones were evaluated for each protease (n = 2). (b) Relative SLC25A38 endogenous levels at different CHX treatment time points in non-targeting sgAAVS1 control and two YME1L1 KO clones, normalized to the protein abundance at 0 hrs (n = 3). Schematic diagram of for degradation of SLC25A38 by YME1L1. Values are mean ± S.D.M.

REFERENCES

1. Bar-Peled, L. and Kory, N., 2022. Principles and functions of metabolic compartmentalization. *Nature metabolism*, *4*(10), pp.1232-1244.
2. Kunji, E.R., King, M.S., Ruprecht, J.J. and Thangaratnarajah, C., 2020. The SLC25 carrier family: important transport proteins in mitochondrial physiology and pathology. *Physiology*, *35*(5), pp.302-327.
3. Shimizu, T., Lengalova, A., Martínek, V. and Martínková, M., 2019. Heme: emergent roles of heme in signal transduction, functional regulation and as catalytic centres. *Chemical Society Reviews*, *48*(24), pp.5624-5657.
4. Yien, Y.Y. and Perfetto, M., 2022. Regulation of heme synthesis by mitochondrial homeostasis proteins. Frontiers in Cell and Developmental Biology, 10, p.895521.
5. Lunetti, P., Damiano, F., De Benedetto, G., Siculella, L., Pennetta, A., Muto, L., Paradies, E., Marobbio, C.M.T., Dolce, V. and Capobianco, L., 2016. Characterization of human and yeast mitochondrial glycine carriers with implications for heme biosynthesis and anemia. *Journal of Biological Chemistry*, *291*(38), pp.19746-19759.
6. Fernández-Murray, J.P., Prykhozhij, S.V., Dufay, J.N., Steele, S.L., Gaston, D., Nasrallah, G.K., Coombs, A.J., Liwski, R.S., Fernandez, C.V., Berman, J.N. and McMaster, C.R., 2016. Glycine and folate ameliorate models of congenital sideroblastic anemia. *PLoS genetics*, *12*(1), p.e1005783.
7. Abu-Zeinah, G. and DeSancho, M.T., 2020. Understanding sideroblastic anemia: an overview of genetics, epidemiology, pathophysiology and current therapeutic options. *Journal of blood medicine*, pp.305-318.
8. Chiabrando, D., Vinchi, F., Fiorito, V., Mercurio, S. and Tolosano, E., 2014. Heme in pathophysiology: a matter of scavenging, metabolism and trafficking across cell membranes. *Frontiers in pharmacology*, *5*, p.61.
9. Cho, N.H., Cheveralls, K.C., Brunner, A.D., Kim, K., Michaelis, A.C., Raghavan, P., Kobayashi, H., Savy, L., Li, J.Y., Canaj, H. and Kim, J.Y., 2022. OpenCell: Endogenous tagging for the cartography of human cellular organization. *Science*, *375*(6585), p.eabi6983.
10. Wang, Y., Yen, F.S., Zhu, X.G., Timson, R.C., Weber, R., Xing, C., Liu, Y., Allwein, B., Luo, H., Yeh, H.W. and Heissel, S., 2021. SLC25A39 is necessary for mitochondrial glutathione import in mammalian cells. *Nature*, *599*(7883), pp.136-140.
11. Shi, X., Reinstadler, B., Shah, H., To, T.L., Byrne, K., Summer, L., Calvo, S.E., Goldberger, O., Doench, J.G., Mootha, V.K. and Shen, H., 2022. Combinatorial G x G x E CRISPR screen identifies SLC25A39 in mitochondrial glutathione transport linking iron homeostasis to OXPHOS. *Nature Communications*, *13*(1), p.2483.
12. Liu, Y., Liu, S., Tomar, A., Yen, F.S., Unlu, G., Ropek, N., Weber, R.A., Wang, Y., Khan, A., Gad, M. and Peng, J., 2023. Autoregulatory control of mitochondrial glutathione homeostasis. *Science*, *382*(6672), pp.820-828.

13. Shi, X., DeCiucis, M., Grabinska, K.A., Kanyo, J., Liu, A., Lam, T.T. and Shen, H., 2024. Dual regulation of SLC25A39 by AFG3L2 and iron controls mitochondrial glutathione homeostasis. *Molecular Cell*, *84*(4), pp.802-810.
14. Morgenstern, M., Peikert, C.D., Lübbert, P., Suppanz, I., Klemm, C., Alka, O., Steiert, C., Naumenko, N., Schendzielorz, A., Melchionda, L. and Mühlhäuser, W.W., 2021. Quantitative high-confidence human mitochondrial proteome and its dynamics in cellular context. *Cell metabolism*, *33*(12), pp.2464-2483.
15. Li, J., Cai, Z., Vaites, L.P., Shen, N., Mitchell, D.C., Huttlin, E.L., Paulo, J.A., Harry, B.L. and Gygi, S.P., 2021. Proteome-wide mapping of short-lived proteins in human cells. *Molecular cell*, *81*(22), pp.4722-4735.
16. Kory, N., uit de Bos, J., van der Rijt, S., Jankovic, N., Güra, M., Arp, N., Pena, I.A., Prakash, G., Chan, S.H., Kunchok, T. and Lewis, C.A., 2020. MCART1/SLC25A51 is required for mitochondrial NAD transport. *Science advances*, *6*(43), p.eabe5310.
17. Luongo, T.S., Eller, J.M., Lu, M.J., Niere, M., Raith, F., Perry, C., Bornstein, M.R., Oliphint, P., Wang, L., McReynolds, M.R. and Migaud, M.E., 2020. SLC25A51 is a mammalian mitochondrial NAD+ transporter. *Nature*, *588*(7836), pp.174-179.
18. Girardi, E., Agrimi, G., Goldmann, U., Fiume, G., Lindinger, S., Sedlyarov, V., Srndic, I., Gürtl, B., Agerer, B., Kartnig, F. and Scarcia, P., 2020. Epistasis-driven identification of SLC25A51 as a regulator of human mitochondrial NAD import. *Nature communications*, *11*(1), p.6145.
19. Ahola, S., Langer, T. and MacVicar, T., 2019. Mitochondrial proteolysis and metabolic control. *Cold Spring Harbor Perspectives in Biology*, *11*(7), p.a033936.
20. Deshwal, S., Fiedler, K.U. and Langer, T., 2020. Mitochondrial proteases: multifaceted regulators of mitochondrial plasticity. *Annual review of biochemistry*, *89*, pp.501-528.
21. MacVicar, T., Ohba, Y., Nolte, H., Mayer, F.C., Tatsuta, T., Sprenger, H.G., Lindner, B., Zhao, Y., Li, J., Bruns, C. and Krüger, M., 2019. Lipid signalling drives proteolytic rewiring of mitochondria by YME1L. Nature, 575(7782), pp.361-365.
22. Anand, R., Wai, T., Baker, M.J., Kladt, N., Schauss, A.C., Rugarli, E. and Langer, T., 2014. The i-AAA protease YME1L and OMA1 cleave OPA1 to balance mitochondrial fusion and fission. *Journal of Cell Biology*, *204*(6), pp.919-929.
23. Rainbolt, T.K., Lebeau, J., Puchades, C. and Wiseman, R.L., 2016. Reciprocal degradation of YME1L and OMA1 adapts mitochondrial proteolytic activity during stress. *Cell reports*, *14*(9), pp.2041-2049.
24. Guernsey, D.L., Jiang, H., Campagna, D.R., Evans, S.C., Ferguson, M., Kellogg, M.D., Lachance, M., Matsuoka, M., Nightingale, M., Rideout, A. and Saint-Amant, L., 2009. Mutations in mitochondrial carrier family gene SLC25A38 cause nonsyndromic autosomal recessive congenital sideroblastic anemia. *Nature genetics*, *41*(6), pp.651-653.
25. Nilsson, R., Schultz, I.J., Pierce, E.L., Soltis, K.A., Naranuntarat, A., Ward, D.M., Baughman, J.M., Paradkar, P.N., Kingsley, P.D., Culotta, V.C. and Kaplan, J., 2009. Discovery of genes essential for heme biosynthesis through large-scale gene expression analysis. *Cell metabolism*, *10*(2), pp.119-130.

ACKNOWLEDGEMENT

We thank all members of the Kory lab for helpful discussion. This work was supported by R35/MIRA GM151097 (N.K.) and a A*STAR fellowship (S.T.).

AUTHOR CONTRIBUTIONS

NK and ST conceptualized the study and wrote the manuscript. ST performed and analyzed experiments.

Figure 1

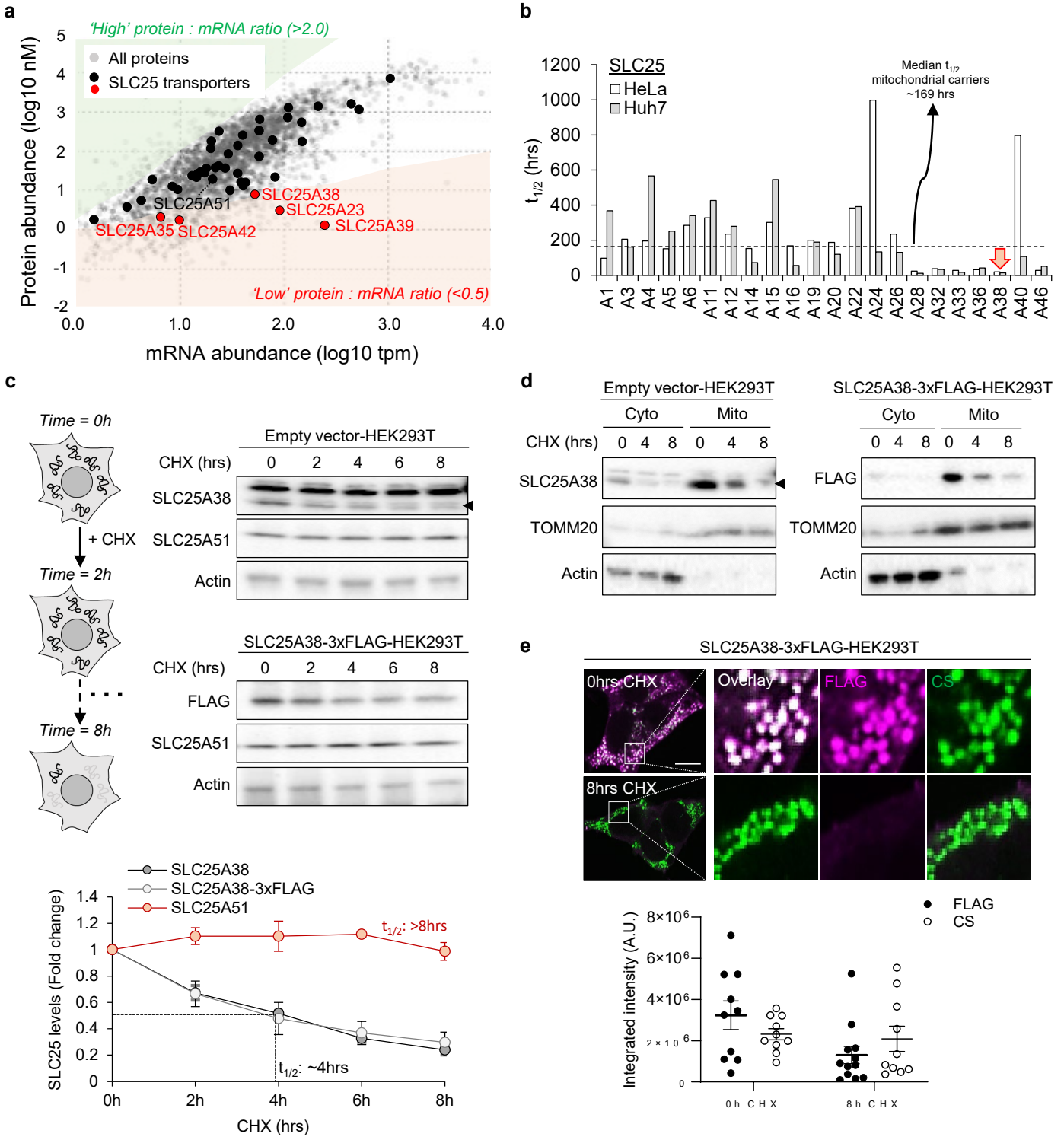
a
'High' protein : mRNA ratio (>2.0)
All proteins
SLC25 transporters
SLC25A51
SLC25A38
SLC25A23
SLC25A39
SLC25A35
SLC25A42
'Low' protein : mRNA ratio (<0.5)
Protein abundance (log10 nM)
mRNA abundance (log10 tpm)
b
SLC25
HeLa
Huh7
Median t1/2 mitochondrial carriers ~169 hrs
t1/2 (hrs)
A1 A3 A4 A5 A6 A11 A12 A14 A15 A16 A19 A20 A22 A24 A26 A28 A32 A33 A36 A38 A40 A46
c
Time = 0h
+ CHX
Time = 2h
Time = 8h
Empty vector-HEK293T
CHX (hrs) 0 2 4 6 8
SLC25A38
SLC25A51
Actin
SLC25A38-3xFLAG-HEK293T
CHX (hrs) 0 2 4 6 8
FLAG
SLC25A51
Actin
SLC25A38
SLC25A38-3xFLAG
SLC25A51
t1/2: >8hrs
t1/2: ~4hrs
SLC25 levels (Fold change)
CHX (hrs)
d
Empty vector-HEK293T
SLC25A38-3xFLAG-HEK293T
Cyto
Mito
CHX (hrs) 0 4 8 0 4 8
SLC25A38
FLAG
TOMM20
Actin
e
SLC25A38-3xFLAG-HEK293T
0hrs CHX
8hrs CHX
Overlay
FLAG
CS
Integrated intensity (A.U.)
0 h CHX
8 h CHX

Figure 2

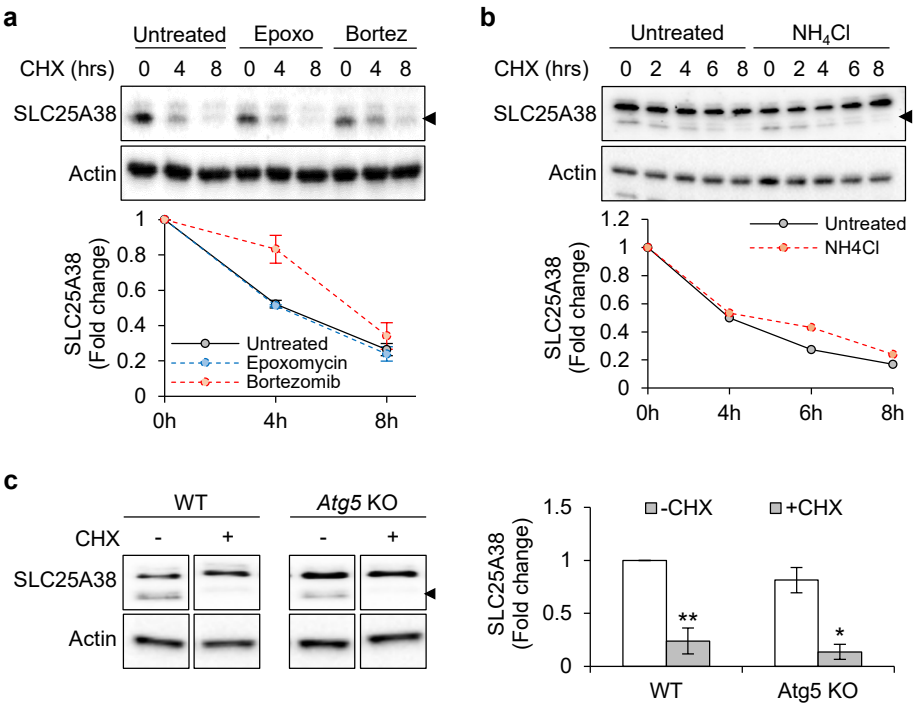
a
Untreated
Epoxo
Bortez
CHX (hrs)
0 4 8 0 4 8 0 4 8
SLC25A38
Actin
SLC25A38 (Fold change)
1
0.8
0.6
0.4
0.2
0
Untreated
Epoxomycin
Bortezomib
0h
4h
8h
b
Untreated
NH4Cl
CHX (hrs)
0 2 4 6 8 0 2 4 6 8
SLC25A38
Actin
SLC25A38 (Fold change)
1.2
1
0.8
0.6
0.4
0.2
0
Untreated
NH4Cl
0h
4h
6h
8h
c
WT
Atg5 KO
CHX
-
+
-
+
SLC25A38
Actin
SLC25A38 (Fold change)
1.5
1
0.5
0
-CHX
+CHX
**
*
WT
Atg5 KO

Figure 3

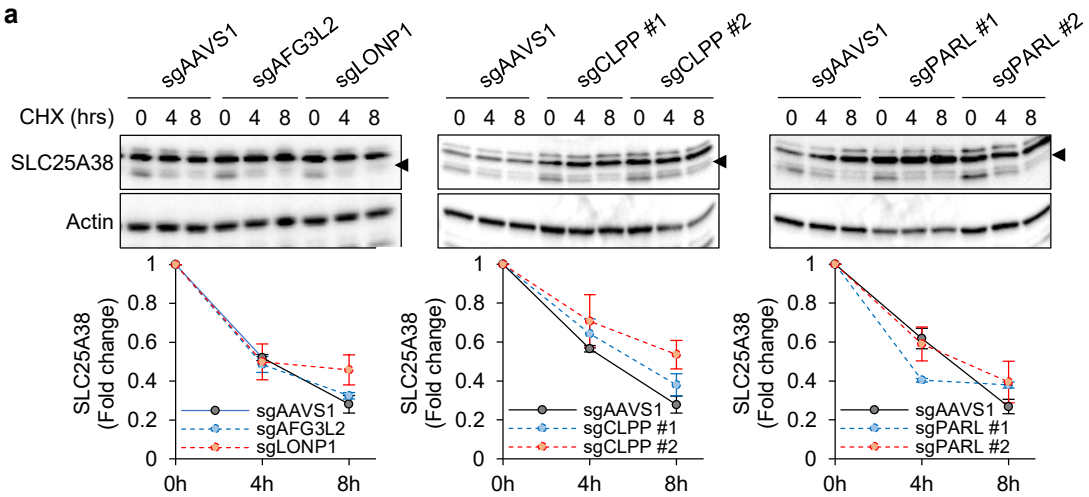
a
sgAAVS1
sgAFG3L2
sgLONP1
sgCLPP #1
sgCLPP #2
sgPARL #1
sgPARL #2
CHX (hrs)
0 4 8 0 4 8 0 4 8
SLC25A38
Actin
SLC25A38 (Fold change)
0h
4h
8h

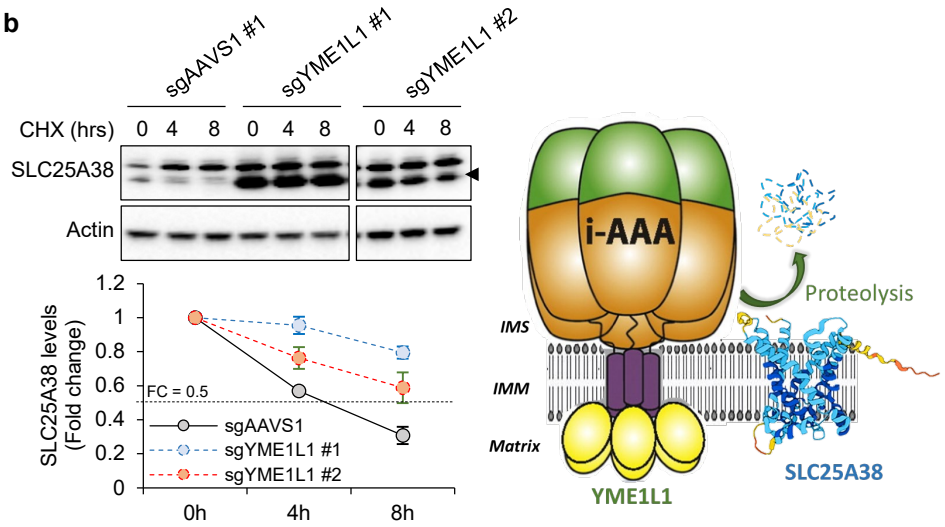
b
sgAAVS1 #1
sgYME1L1 #1
sgYME1L1 #2
CHX (hrs)
0 4 8 0 4 8 0 4 8
SLC25A38
Actin
SLC25A38 levels (Fold change)
FC = 0.5
0h
4h
8h
i-AAA
Proteolysis
IMS
IMM
Matrix
YME1L1
SLC25A38